Journal of Cancer Research and Clinical Oncology (2025) 151:136
https://doi.org/10.1007/s00432-025-06183-0

RESEARCH

Low-intensity pulsed ultrasound affects proliferation and migration of human hepatocellular carcinoma cells

Mingzhen Yang[1,2] · Zhihui Lu[1] · Bangzhong Liu[1] · Guanghua Liu[1] · Mingfang Shi[1] · Ping Wang[1]

Received: 3 November 2024 / Accepted: 24 March 2025 / Published online: 10 April 2025

Abstract

Purpose Low-intensity pulsed ultrasound (LIPUS) is an effective ancillary treatment modality for various malignancies. However, the mechanisms underlying the role of LIPUS in cancer treatment have not been fully elucidated. We investigated the effects and underlying mechanism of LIPUS on the proliferation, apoptosis, migration, and invasion of hepatocellular carcinoma (HCC) cells.

Methods The HCC cell lines SMMC7721 and HCCLM3 were exposed to 1 MHz LIPUS at intensities of 0.5, 1.0, 1.5 W/cm^2 for 60 s. Cell morphology, viability, apoptosis, colony formation, migration, and invasion were assessed. Intracellular reactive oxygen species (ROS) levels and mitochondrial membrane potential were evaluated using a ROS assay kit and a JC-1 staining kit. Western blotting was performed to quantify changes in matrix metallopeptidases and epithelial-mesenchymal transition-related proteins. Orthotopic Hep3B-Luc tumor-bearing mice were treated with LIPUS at 1.5 W/cm^2 or 0 W/cm^2 and growth trend was measured.

Results The results showed that different intensities of ultrasound affected cellular activity, inhibited cell proliferation and cloning, facilitated intracellular cytoskeletal protein reorganization, and induced cell apoptosis, particularly at the intensity of 1.5 W/cm^2, through the ROS/mitochondria pathway. LIPUS enhanced SMCC7721 and HCCLM3 cell migration and invasion in a dose-dependent manner by regulating matrix metallopeptidases and epithelial-mesenchymal transition-related proteins. In vivo experiments confirmed the inhibitory effect of LIPUS at 1.5 W/cm^2 on tumor growth.

Conclusions Although LIPUS induced cell apoptosis and inhibited cell proliferation, it also promoted the invasion and metastasis of HCC cells under certain conditions, which was related to the regulation of matrix metallopeptidases and epithelial-mesenchymal transition-related proteins.

Keywords Apoptosis · Epithelial-mesenchymal transition · Hepatocellular carcinoma · Low-intensity pulsed ultrasound

Abbreviations

LIPUS	Low intensity pulsed ultrasound
HCC	Hepatocellular carcinoma
CCK-8	Cell Counting Kit-8
OD	Optical density
ROS	Reactive oxygen species
MMP	Mitochondrial membrane potential
EMT	Epithelial-mesenchymal transition
MMPs	Matrix metallopeptidases

Introduction

Ultrasound serves both diagnostic and therapeutic purposes in current clinical practice. In particular, low-intensity pulsed ultrasound (LIPUS), a type of medium-frequency ultrasound characterized by a pulse-wave mode output and significantly lower intensity delivery, has gained momentum owing to its broad potential applications in the fields of oncology, regeneration, and rehabilitation (Ikai et al. 2008;

Mingzhen Yang and Zhihui Lu contributed equally to this work.

✉ Mingfang Shi
shi.mingfang@zs-hospital.sh.cn

✉ Ping Wang
wang.ping8@zs-hospital.sh.cn

[1] Department of Rehabilitation, Zhongshan Hospital, Fudan University, Shanghai 200032, China

[2] Shanghai Institute of Rehabilitation with Integrated Western and Chinese Traditional Medicine, Shanghai 200032, China

Jiang et al. 2019). For instance, LIPUS has been previously used for sonodynamic therapy, ultrasound-mediated chemotherapy, sonoporation, gene delivery or transfection, muscle and tendon repair, and bone tissue regeneration (Urita et al. 2013; Xin et al. 2016). In the field of cancer, available evidence from both in vitro and in vivo studies suggests that LIPUS is effective in treating various types of malignancies such as glioma(Habashy et al. 2024), osteosarcoma(Sawai et al. 2012), leukemia(Buldakov et al. 2015), and hepatocellular carcinoma (HCC)(Shi et al. 2016), either alone or in combination with other therapeutic strategies. Although preliminary studies have suggested that the therapeutic efficacy of LIPUS is largely related to its thermal and nonthermal effects(Tang et al. 2015), the cellular and molecular mechanisms underlying its biological effects remain unknown and warrant further investigation.

HCC, the most common primary liver cancer, is the 6th most common neoplasm and the 3rd leading cause of cancer-related mortality, with an annual incidence of 782,000 cases and 746,000 deaths worldwide(Vogel et al. 2022). Surgical resection, chemotherapy, and radiotherapy are the main therapeutic modalities for HCC. Despite the implementation of various management regimens for HCC treatment, prognosis remains extremely poor owing to the high likelihood of metastasis(Tan et al. 2018; Huang et al. 2020). Cancer spread involves steps such as invading tissues, breaking away from the original tumor site, entering blood vessels, surviving in the bloodstream, transitioning in and out of dormancy, adapting to new environments at distant sites, promoting new blood vessel growth, and evading immune system detection(Ganesh and Massagué 2021; Castaneda et al. 2022; Fares et al. 2020). Previous studies have highlighted that disruption of endoplasmic reticulum homeostasis and aspartate metabolism reprogramming play pivotal roles in HCC survival and distant metastasis(Hu et al. 2023a, b; Chen et al. 2022a, b). Moreover, epithelial-mesenchymal transition (EMT) facilitated by imbalanced matrix metalloproteinases (MMPs) has been implicated in HCC metastasis(Scheau et al. 2019).

LIPUS stimulation, either alone or in combination with chemotherapeutic drugs, has been widely accepted to produce improved synergistic anti-tumor effects(Lopez et al. 2021; Tamboia et al. 2022; Cao et al. 2021). Preliminary in vivo and in vitro studies have shown that LIPUS can increase the permeability of the plasma membrane and improve the effects of anticancer drugs without damaging the whole cell (Liu et al. 2019; Jain et al. 2018). We have previously reported that LIPUS induced apoptosis of SMMC-7721 human HCC cells in vitro and that apoptosis resulted from the initiation of the following pathways: direct and indirect damage to DNA in cell nuclei, the Ca^{2+} pathway, and the mitochondrial pathway, which converge at the point of caspase-3 activation(Shi et al. 2016). These findings validated the potential role of LIPUS in the treatment of liver cancer.

However, the exact effects and molecular mechanisms of LIPUS on HCC remain largely unknown. Therefore, the purpose of this in vitro study was to investigate the effects of different LIPUS intensities on the apoptosis, proliferation, and migration of HCC cells.

Materials and methods

Cells and cell culture

The HCC cell lines SMCC7721 and HCCLM3 were provided by the Liver Cancer Research Institute of Zhongshan Hospital (Shanghai, China). Cells were cultured in Dulbecco's Modified Eagle's Medium (DMEM; Gibco, Thermo Fisher, USA) supplemented with 10% fetal bovine serum (Gibco, Thermo Fisher), 100U/ml penicillin and 100 mg/ml streptomycin (Gibco, Thermo Fisher) at 37°C in a thermostatic incubator with 5% CO_2. Cells were seeded into T-25cm^2 culture flasks (Corning, NY, USA) for 24 h prior to LIPUS experiments. The cell viability was greater than 95% before exposure, as assessed by trypan blue staining.

LIPUS setup and cell treatment

The LIPUS setup was similar to that described in our previous report(Shi et al. 2016). Briefly, the ultrasonic transducer BTL-5000 (BTL Industries Limited, United Kingdom) was operated at a frequency of 1 MHz. The experimental transducer parameters were as follows: repetition frequency, 100 Hz; sonication duration, 60s; and DF, 25%. The ultrasonic transducer was secured using a clamp attached to a metal stand to ensure vertical irradiation. A coupling agent was used at the interface between the transducer surface and culture plate to minimize air interference. The contact area of the transducer was aligned well with that of the cell culture dish.

HCC cells in the logarithmic growth phase were dissociated and resuspended in the culture medium at a concentration of 1×10^5/ml. HCC cells formed a monolayer on the bottom of 6-well culture plates with a surface area of 5 cm^2, and the thickness of the well bottom was 1.3 mm. The cell culture medium (2 mL) was added to achieve a final depth of approximately 5 mm. The 5 cm^2 ultrasound transducer was fixed to the bottom of the culture plate with a coupling gel (depth < 1 mm) for optimal acoustic matching.

The HCC cell lines SMMC7721 and HCCLM3 were exposed to 1 MHz LIPUS at different intensities (0.5, 1.0, 1.5 W/cm^2) for 60 s. The control cells were placed similarly,

but without actual LIPUS exposure. Cells were collected for further testing after sonication under sterile conditions, and each treatment was independently replicated five times.

Measurement of cell viability

Cell viability was assessed using the trypan blue dye exclusion test as described by Feril et al.(Feril et al. 2005). An equal volume of 0.3% trypan blue solution (Beyotime, China) in PBS was added to 100 µL cell suspension. After incubation at room temperature for 5 min, the viable and non-viable cells were counted using a hemocytometer. The percentage of viable cells was calculated as the ratio of viable cells to the total number of cells.

Cell morphology and cytoskeletal proteins

Characteristic micrographs of SMMC7721 and HCCLM3 cells exposed to 1 MHz LIPUS at different intensities (0, 0.5, 1.0, 1.5 W/cm^2) for 60 s were examined under a microscope. The cytoskeletal protein F-actin was detected by fluorescence staining with an F-actin staining reagent (Abcam, Burlingame, CA, USA). A green fluorescent working reagent was prepared by combining Agent A and Agent B in a ratio of 1:1 and incubated with the cells in a 6-well plates at 25℃ for 15–60 min. The fluorescent reagent was removed, and the adherent cells were washed several times. The prepared cells were visualized using fluorescence microscopy and the cytoskeleton was photographed.

Detection of apoptosis

The Annexin V-FITC apoptosis detection kit (BD Biosciences, San Jose, CA, USA) was used to detect apoptosis according to the manufacturer's instructions. Briefly, cells were trypsinized and collected after 6 h of incubation. The cells were then stained with fluorescein isothiocyanate-labeled annexin V and propidium using a binding buffer at room temperature for 10 min in the dark. Finally, flow cytometric analysis was performed using a FACSCalibur instrument (BD Biosciences).

Measurement of cell proliferation

The Cell Counting Kit (CCK)-8 (Dojindo Laboratories, Japan) was used to detect the growth or proliferation of SMCC7721 and HCCLM3 cells after LIPUS sonication. The absorbance at 450 nm was measured using a microplate reader, and the optical density (OD) was recorded.

For the colony formation assay, LIPUS-treated cells were seeded in 6-well plates at 800 cells/well. After incubation in a humidified incubator at 37℃ for 7–10 days, depending on the characteristics of the cell line, the cells were fixed with 4% paraformaldehyde for 30 min and then stained with crystal violet staining solution for another 30 min. Finally, both the control and experimental groups were counted and imaged to determine the number of HCC cell colonies.

Measurement of intracellular ROS

Intracellular ROS levels were assessed by staining cells with 2,7-DCF-diacetate using a ROS assay kit (Beyotime Biotech, China) according to the manufacturer's instructions. Briefly, cells were exposed to 10µ M DCFH-DA for 30 min and washed twice with PBS before analysis under a fluorescence microscope. To investigate inhibitory effects, cell viability was measured in response to LIPUS at 1.5 W/cm^2 in the presence of the specific ROS scavenger NAC at a concentration of 5 µM that did not damage cultured cells.

Assessment of mitochondrial membrane potential (MMP)

MMP was evaluated using a JC-1 staining kit (Keygen Biotech Co., China) according to the manufacturer's instructions. Briefly, cells were incubated with 5 µg/ml JC-1 in 1 ml of working solution for 30 min at 37℃ in the dark. After two washes with PBS, fluorescence images were captured using a fluorescence microscope, as previously described.

Migration and invasion assay

The surviving HCC cells maintained in culture for 24 h post-sonication were harvested and subjected to Transwell migration and invasion assays to evaluate their metastatic potential. For migration assays, approximately 10^4 tumor cells were seeded in the upper chamber of a transwell insert and placed in one well of a 24-well plate containing 500 µL DMEM supplemented with 30% FBS. The cells were incubated for 48 h at 37 °C in a humidified atmosphere containing 5% CO^2. After incubation, the cells in the upper chamber were fixed with 4% paraformaldehyde (Beyotime) for 30 min and stained with crystal violet (Beyotime) for another 30 min.

For the invasion assays, equal numbers of tumor cells were seeded on Matrigel-coated chambers (50 µL; BD Biosciences) and incubated at 37℃ for 3 h. The number of cells that invaded or migrated through the chamber membrane was quantified under a ×200 microscope. Each group was tested in quintuplicate, and the experiments were independently repeated at least three times.

Analysis of matrix metallopeptidases (MMPs) and EMT-associated protein

Western blot analysis was performed to quantify the changes in EMT-associated proteins, including E-cadherin, N-cadherin, Snail, Slug, Vimentin and Twist. In addition, MMP-2 and MMP-9 levels were evaluated.

Animal experiments

Female BALB/c mice aged 6–8 weeks were purchased for the preliminary experiments. Orthotopic Hep3B-Luc tumor-bearing mouse model was established by inoculating 4×10^6 Hep3B-Luc tumor cells into the livers of BALB/c mice. Two weeks after modeling, the mice were divided into two groups with six mice in each group. The mice in ultrasound treatment group were exposed to 1 MHz LIPUS at 1.5 W/cm² for 60s once daily for 7 days. The control group was subjected to sham stimulation with a treatment intensity of 0 W/cm². The Lumina II in vivo imaging system was used to record the bioluminescence signals of the entire animal until 3 weeks post-ultrasound treatment. Changes in body weight and tumor growth were monitored. At the end of the experiment, the liver and tumor weights were measured, and lung tissues were subjected to hematoxylin and eosin (H&E) staining to observe tumor metastasis. All animal experiments were approved by the Ethics Review Committee of Zhongshan Hospital, Fudan University.

Statistical analysis

Experiments were performed in triplicate; real-time measurements were obtained and numerical data are presented as mean ± standard deviation. Statistical analysis was performed using Student's t-test and one-way ANOVA, and significance was set at $p < 0.05$.

Results

In the present study, we investigated the effects of LIPUS on human HCC cells. Specifically, we assessed the apoptosis-inducing potential of LIPUS in the SMMC-7721 and HCCLM3 cell lines, explored alternative mechanisms associated with tumor cell apoptosis, and evaluated its impact on HCC cell proliferation and invasion.

Effects of LIPUS on cell viability and structural changes

First, we examined the effects of LIPUS on the cell viability and structure. We observed an intensity-dependent reduction in the viability of both SMMC7721 and HCCLM3 cells following LIPUS treatment. The highest inhibition was achieved at an acoustic intensity of 1.5 W/cm^2 (up to 61% inhibition compared to the controls, $p < 0.001$). No significant changes in cell viability were observed at an intensity of 0.5 W/cm^2 for either SMMC7721 or HCCLM3 (3% and 4% inhibition compared to controls for SMMC7721 and HCCLM3, respectively; see Fig. 1). Similar results were observed for the proliferation capacity and clonogenicity (Fig. 2). The acoustic intensity of 1.5 W/cm^2 had the most significant inhibitory effect on the ability of both SMMC7721 and HCCLM3 cells to proliferate and form colonies.

Under light microscopy, the cells exposed to LIPUS showed morphological changes from elliptical to narrow. In addition, intercellular tight junctions were disrupted, resulting in the loosening of individual cell layers. Over time, these cells exhibited distinct morphological features consistent with those of apoptotic cells such as nuclear condensation, loss of cell membrane integrity, and cellular debris (Fig. 1).

Migratory ability is related to the actin cytoskeleton, which maintains the polarity of cells, is essential for normal tissue homeostasis, and its disruption can lead to tumor metastasis(Ortiz et al. 2021). Staining with the green fluorescent protein F-actin showed that the cell morphology appeared rounded, and the edges were smooth in the control group; the connections between cells were tight and palisaded. However, in the LIPUS-treated groups, particularly at 1.0 W/cm^2 and 1.5 W/cm^2, distinct changes in cell morphology from palisade-like to fiber-like were observed. Narrow tentacle-like edges were observed in individual cells, and the connections between cells appeared loose (Fig. 3). These changes indicate that LIPUS treatment induces the reorganization of actin bundles, increasing the HCC polarity and filopodia-like protrusions.

LIPUS induces apoptosis in HCC

We measured the apoptosis index using flow cytometry to determine whether the growth inhibition observed in LIPUS-treated cells was associated with the induction of apoptotic cell death. The results showed that LIPUS treatment at an intensity of 1.5 W/cm^2 induced apoptosis in both SMMC7721 and HCCLM3 cells in an intensity-dependent manner (6.81% and 8.99% of apoptotic cells compared to controls for SMMC7721 and HCCLM3 cells, respectively; $p < 0.001$; Fig. 4). However, no significant difference in apoptosis between the group treated with LIPUS at 0.5 W/cm^2 and the control group was observed (0.55% vs. 0.41% for SMMC7721; 4.84% vs. 4.21% for HCCLM3). In the in vivo experiments, we also observed the inhibitory effect of

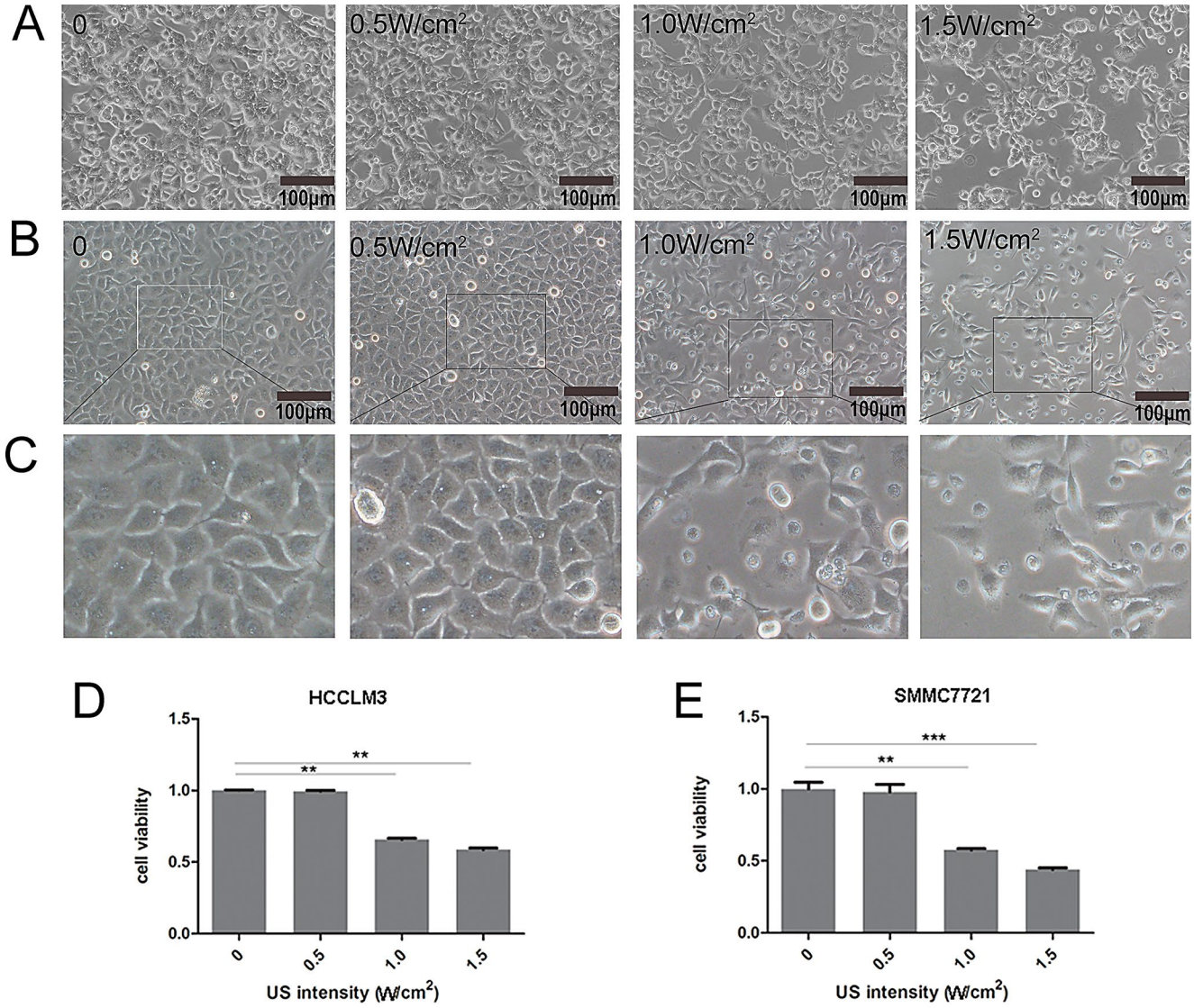

Fig. 1 The morphological characteristics and cell viability of SMMC7721 and HCCLM3 cells after LIPUS exposure. HCCLM3 (**A**) and SMMC7721 (**B**) cells were treated with LIPUS at different irradiation intensities, including control, 0.5, 1.0, and 1.5 W/cm^2 for 30s each. (Scale bar = 100 μm). (**C**) Partially magnified image. The trypan blue assay was used to evaluate the viability of HCCLM3 (**D**) and SMMC7721 (**E**) cells induced by LIPUS at different intensities. LIPUS at an intensity of 1.0 W/cm^2 and 1.5 W/cm^2 showed a significant inhibitory effect on cell viability. Data are presented as mean ± SD ($n = 5$); $^{**}p < 0.01$, $^{***}p < 0.001$

LIPUS on tumor growth, which was most pronounced on the 7th day of treatment ($P = 0.045$) (Fig. 10C).

ROS overproduction has been proposed as a key factor for damaging cellular components and inducing apoptosis in tumor cells(Caillot et al. 2020). Previous studies have shown that sonodynamic treatment induces cellular damage through ROS generation(Loke et al. 2023; Son et al. 2020; Liang et al. 2020). To confirm the apoptotic mode of cancer cell death observed in this study, oxidative stress generated by LIPUS treatment was determined under different treatment conditions. As shown in Fig. 5A and B, ROS production significantly increased in both SMMC7721 and HCCLM3 cells after LIPUS irradiation, particularly at intensities of 1.5 W/cm^2. To further explore the relationship between ROS generation and HCC cell viability under LIPUS treatment at an intensity of 1.5 W/cm^2, the ROS scavenger NAC was administered prior to treatment. LIPUS treatment resulted in a reduction in cell viability in both SMMC7721 and HCCLM3 cells, which was reversed by pretreatment with NAC (Fig. 5C). These results suggested that ROS may be involved in mediating the apoptotic effects of LIPUS.

MMP pore formation and subsequent mitochondrial membrane depolarization are critical events in the initiation of apoptosis involving the mitochondria. To assess MMP, JC-1 dye was used to evaluate mitochondrial membrane

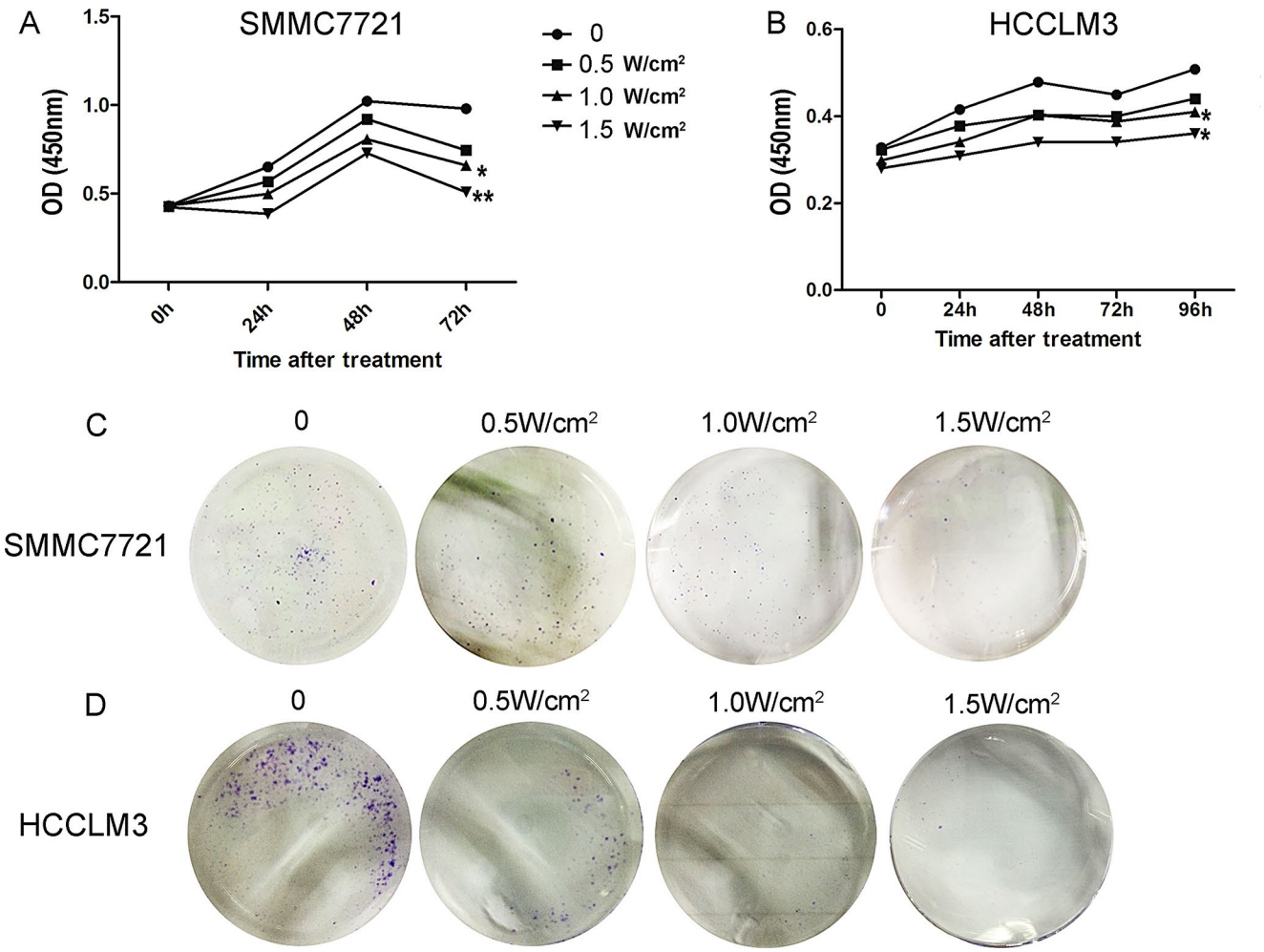

Fig. 2 Effects of LIPUS on HCC cell proliferation. The proliferation of both SMMC7721 (**A**) and HCCLM3 (**B**) was significantly suppressed after LIPUS irradiation at intensities of 0.5 W/cm^2, 1.0 W/cm^2, and 1.5 W/cm^2 compared to that of the control group (0 W/cm^2). Representative images of colony formation efficiency for SMMC7721 (**C**) and HCCLM3 (**D**) cells treated with LIPUS were obtained; CCK8 assay results are presented as optical density ($OD_{450\ nm}$) values. Photographs of colony formation were captured with a camera. * $p<0.05$, ** $p<0.01$)

potential. Cells with intact membranes exhibit bright red fluorescence, indicative of JC-1 aggregates accumulating within substrates with high levels of MMP. A decrease in MMP and subsequent damage to mitochondria is indicated by a small amount of red fluorescence in the cells. As shown in Fig. 6A and B, exposure of both SMMC7721 and HCCLM3 cells to LIPUS at 1.5 W/cm^2 resulted in almost no red fluorescence, suggesting that decreased MMP may serve as a specific signal for LIPUS-induced HCC cell apoptosis.

LIPUS enhances cell migration and invasion in a dose-dependent manner

In vitro, a significantly higher number of HCCLM3 cells exposed to ultrasound at an intensity of 1.5 W/cm^2 migrated through the transwell membrane than the control cells. In SMMC7721 cells, both 1.0 and 1.5 W/cm^2 ultrasound treatment promoted cell migration (Fig. 7). Regarding invasion effects, only the high intensity ultrasound treatment (1.5 W/cm^2) enhanced cell invasion in both cell lines; no significant effect was observed in the groups treated at lower intensity (0.5 and 1.0 W/cm^2) (Fig. 8). In vivo, no lung metastasis was observed during the monitoring period (Fig. 10E). Further exploration of the ultrasound treatment parameters in vivo may be necessary.

LIPUS modulates HCC metastasis through the regulation of MMPs and EMT

MMP2 and MMP9 are widely recognized as the proteins most closely associated with HCC metastasis. Our results indicated that LIPUS may promote the metastasis of adherent

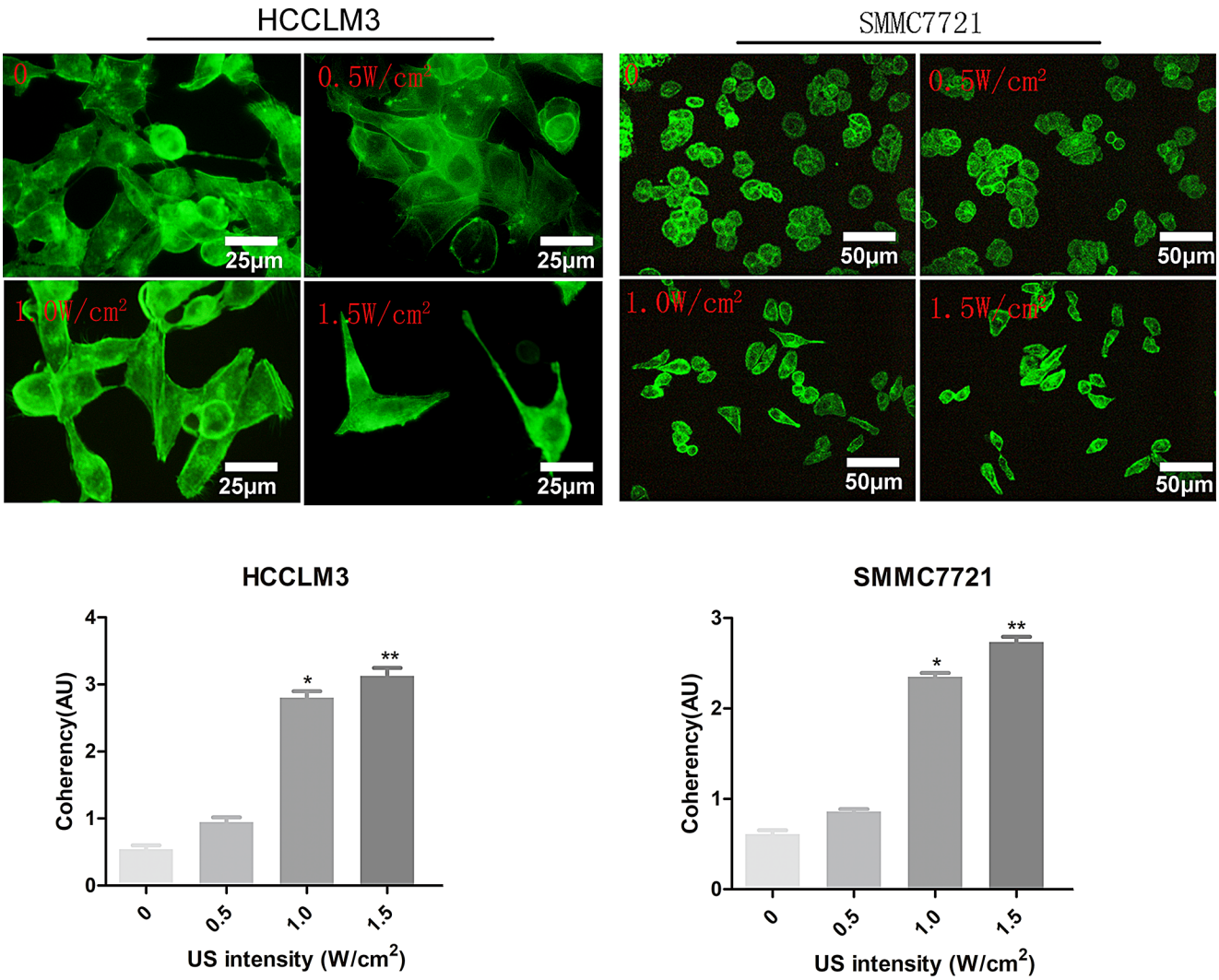

Fig. 3 The arrangement of the cytoskeletal protein F-actin was changed after LIPUS treatment. The cells were stained green and observed under fluorescence microscopy. The morphology changed from palisade to fiber in both HCCLM3 and SMMC7721. Coherency of the cytoskeleton was calculated using Orientation J plugin and appeared markedly increased with LIPUS at different intensities, particularly at 1.0 and 1.5 W/cm^2. *$p<0.05$, **$p<0.01$

HCC cells by upregulating MMP2 expression, which was elevated in both HCCLM3 and SMMC7721 cells. In contrast, MMP9 expression was significantly upregulated only in SMMC7721 cells and remained almost unchanged in HCCLM3 cells (Fig. 9A).

Given the morphological effects of LIPUS on HCC SMMC7721 and HCCLM3 cells in vitro, we investigated whether ultrasound irradiation at 1.5 W/cm^2 promoted the metastasis of HCC cells by inducing EMT. E-cadherin expression, a hallmark event of EMT, was downregulated in SMMC7721 cells after exposure to 1.5 W/cm^2 ultrasound (Fig. 9C). In addition, the expression level of the mesenchymal protein N-cadherin was upregulated, and the transcription factors Slug and Twist, which are involved in EMT control, correspondingly increased in SMMC7721 cells after irradiation at 1.5 W/cm^2. Similar results of E-cadherin and N-cadherin were observed in HCCLM3, but the trend was not statistically significant. Vimentin expression significantly increased along with the upregulation of the Slug transcription factor involved in the EMT process. Our results suggest that LIPUS irradiation at 1.5 W/cm^2 may promote the metastasis of HCC cells, particularly in SMMC7721 cells, through EMT.

Discussion

LIPUS plays a key role in targeted chemotherapy, direct release of anticancer drugs, and induction of apoptosis and necrosis in cells. LIPUS treatment enhances drug uptake by

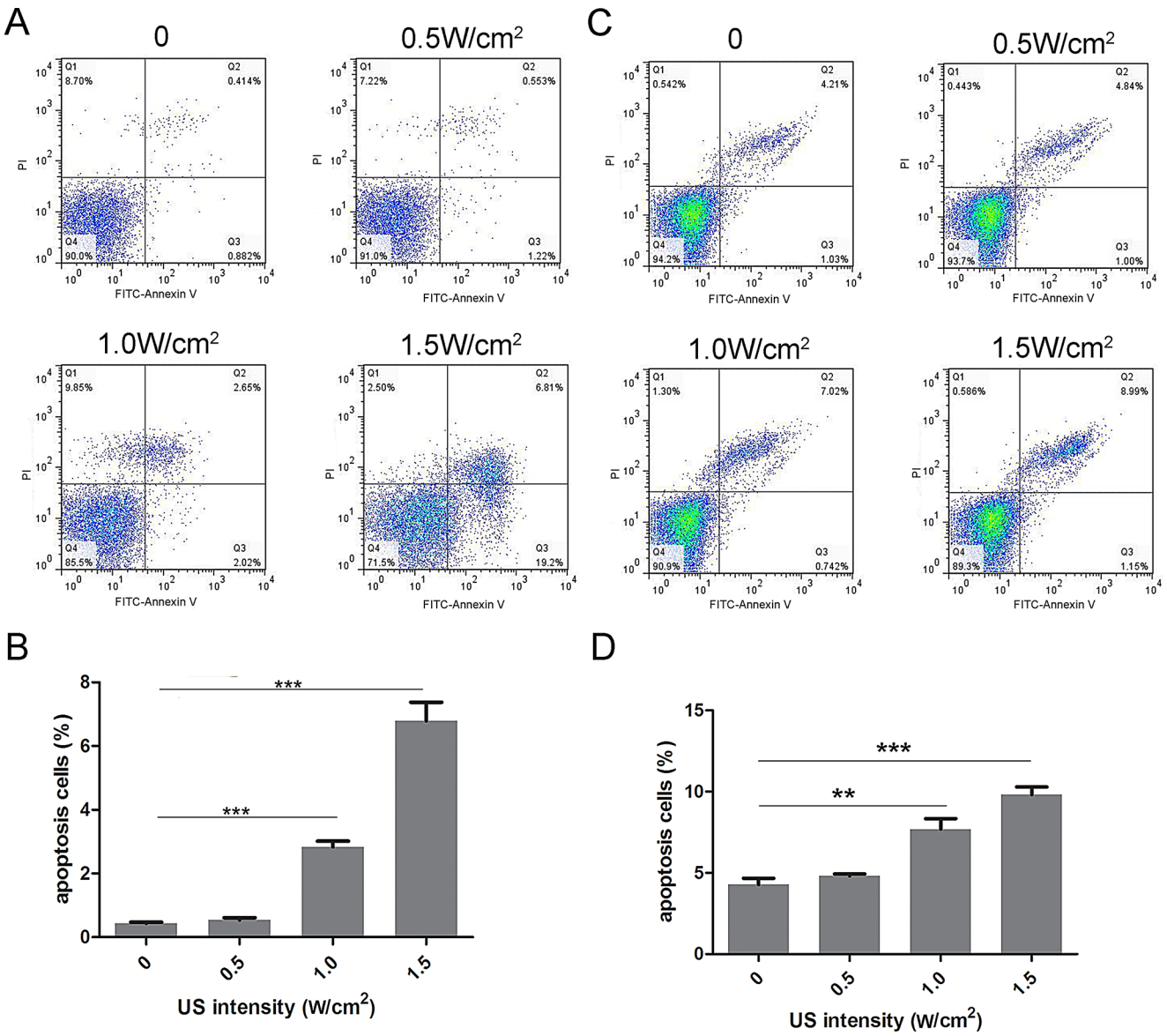

Fig. 4 Analysis of apoptosis rate in HCC cells. Flow cytometric analysis of apoptosis was performed on both SMMC7721 (**A**) and HCCLM3 (**C**) cells after LIPUS treatment at intensities of 0.5, 1.0, and 1.5 W/cm^2 compared to the control group (0 W/cm^2). Apoptotic levels were significantly higher in the 1.5 W/cm^2 and 1.0 W/cm^2 groups than in the control group for both SMMC7721(**B**) and HCCLM3(**D**) cells, whereas no statistical increase was observed in the 0.5 W/cm^2 group compared to controls. Data are expressed as mean ± SD from five independent experiments. $^{**}p<0.01$, $^{***}p<0.001$

increasing cell membrane permeability through two physical mechanisms: heat and cavitation(Li et al. 2023). Our previous study demonstrated the critical role of the mitochondrial caspase pathway in apoptosis induction in SMMC-7721 cells. In this study, we investigated the potential effects of ultrasound waves on the proliferation and invasion of different hepatoma cell lines. After conducting a series of intensity tests, we found that ultrasound affected HCCLM3 and SMMC-7721 cells in a dose-dependent manner and resulted in the inhibition of liver tumor cell proliferation and the induction of cell apoptosis. However, LIPUS also increased the migration and invasion ability of tumor cells.

Effects of LIPUS on cell viability and structural changes

The activity and proliferation of HCCLM3 and SMMC-7721 cells decreased with an increasing intensity of ultrasound stimulation in vitro, further confirming the inhibitory effect of LIPUS on tumor cell growth. Microscopically, LIPUS treatment induced changes in the cell membrane permeability, cytoplasmic porosity, and cell morphology. Fluorescence microscopy revealed changes in F-actin organization within the cytoskeleton. This is based on the

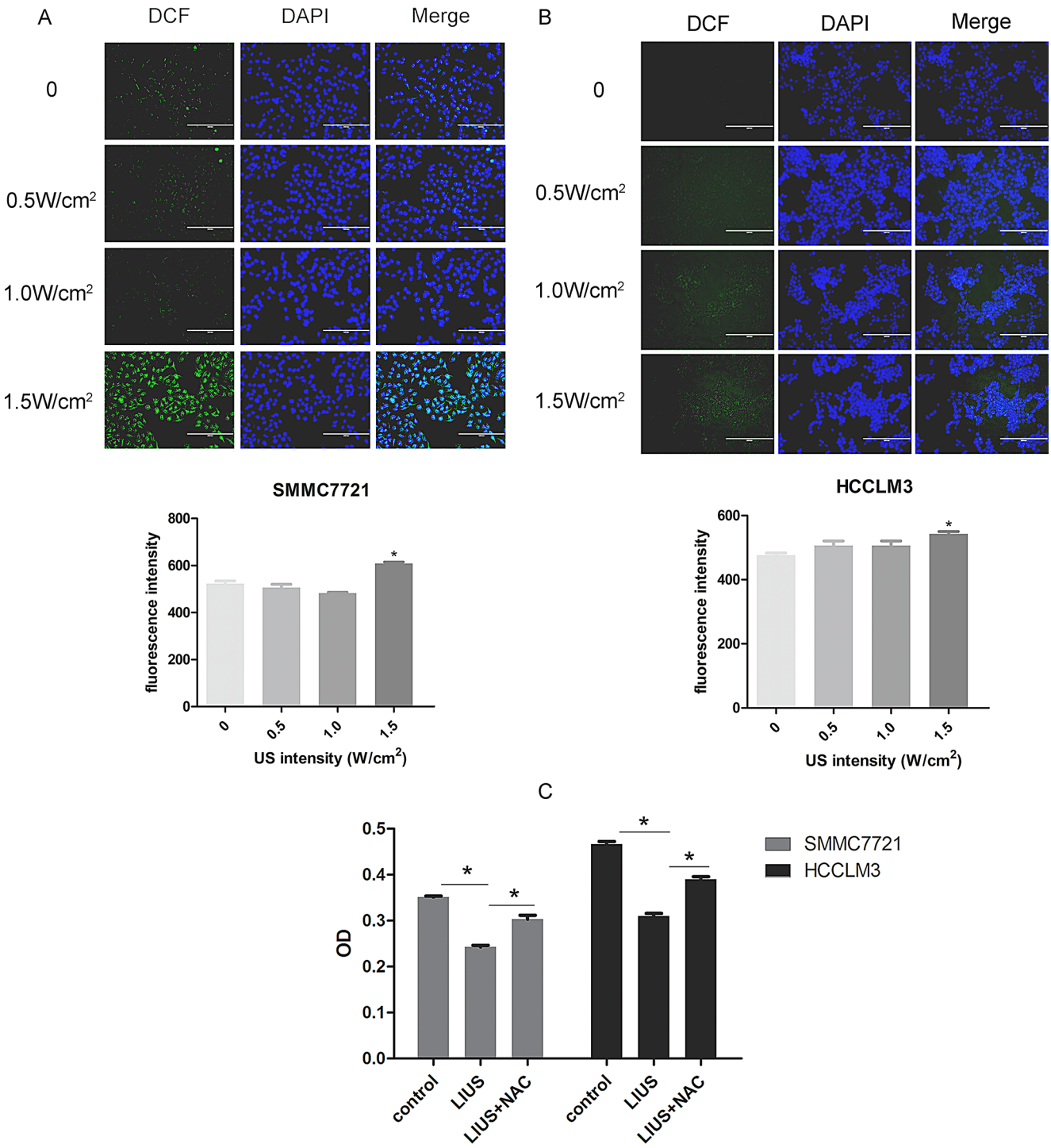

Fig. 5 Effect of LIUPS on ROS generation in HCC cells. Representative images of changes in ROS levels were obtained by immunofluorescence assays for SMMC7721 (**A**) and HCCLM3 (**B**) cells after exposure to LIPUS at intensities of 0.5, 1.0, and 1.5 W/cm^2. (**C**) Cell viability was measured by CCK8 assay in SMMC7721 and HCCLM3 treated with LIPUS at 1.5 W/cm^2 with and without NAC. * $p<0.05$. Scale bar = 100 μm

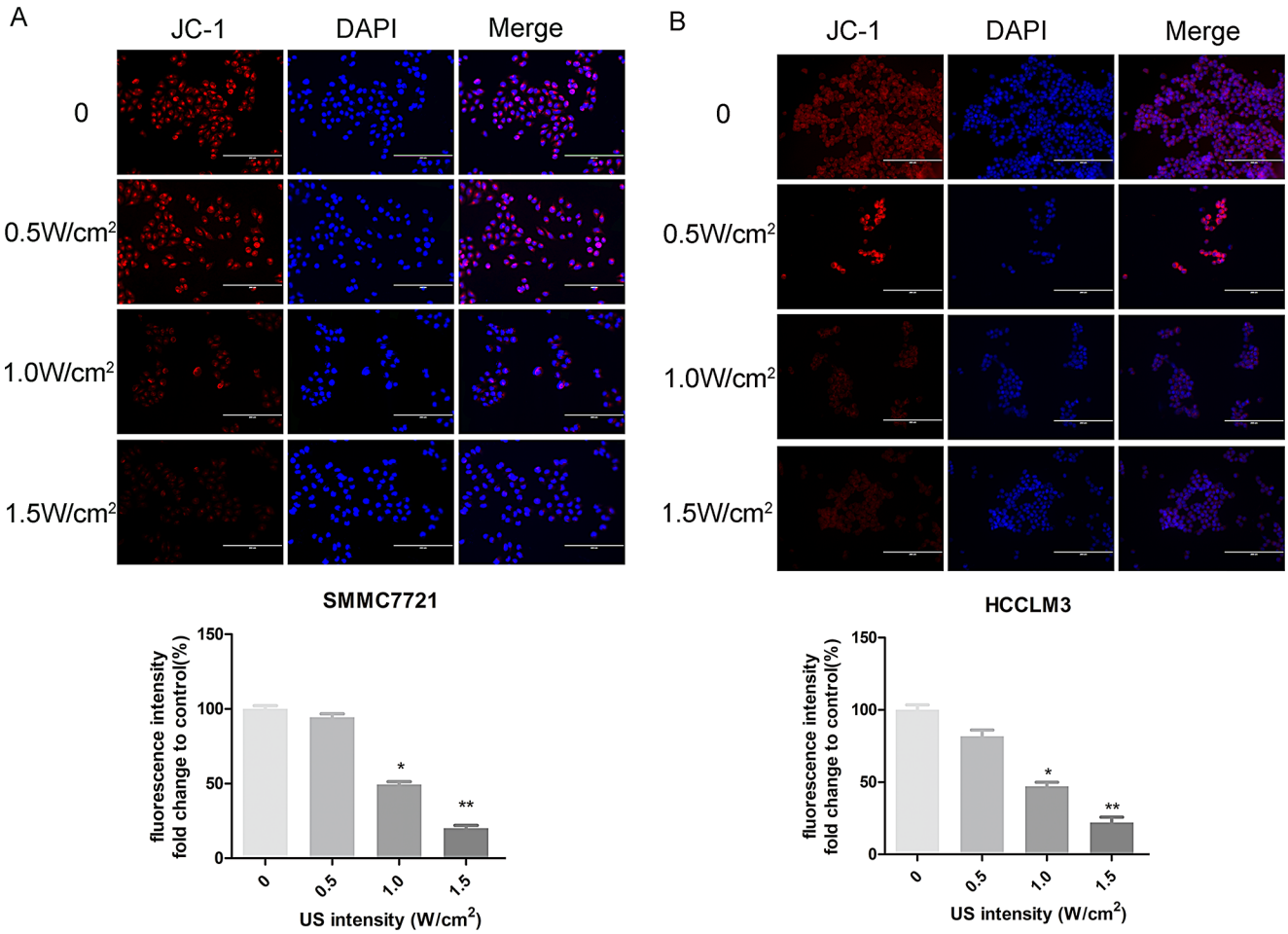

Fig. 6 Effect of LIPUS on MMP reduction in HCC cells. Representative images of JC-1 staining in SMMC7721 (**A**) and HCCLM3 (**B**) are shown. Upon exposure to LIPUS irradiation, the number of cells exhibiting JC-1 probe color decreased; red fluorescence intensity of JC-1 staining reflects the level of MMP dysfunction. *$p<0.05$, **$p<0.01$, Scale bar = 100 μm

notion that ultrasonic waves can induce profound physical and chemical changes in cellular architecture. The observed decrease in cell proliferation can be attributed to cell death resulting from a variety of processes: apoptosis, necrosis, and lysis(Hou et al. 2020; Cotter et al. 1990).

LIPUS induces apoptosis of HCCLM3 and SMMC-7721

Apoptosis is a type of programmed cell death characterized by nuclear condensation and formation of apoptotic bodies. It has become an area of interest in tumor therapy because it induces the natural apoptosis of tumor cells, thereby reducing damage to normal tissues during treatment(Evan and Vousden 2001; Pan et al. 2022). In particular, LIPUS reduced the proliferation of human hepatocellular carcinoma SMMC-7721 and HCCLM3 cells while promoting apoptosis. However, the molecular mechanisms underlying ultrasound-induced apoptosis remain unclear. Current evidence suggests that oxidative damage, dysregulation of calcium homeostasis, and mitochondrial dysfunction are the primary mechanisms involved in the induction of apoptosis(Gupta et al. 2021). Caspase overexpression induces apoptosis in various cell types including cancer cells(Chrysovergis et al. 2019). In addition, the intrinsic mitochondria-mediated apoptotic pathways contribute significantly to this process by activating dysfunctional mitochondria(Chrysovergis et al. 2019).

LIPUS, as a non-invasive sonodynamic therapy, can induce microbubble formation through the process of acoustic cavitation, thereby generating ROS, such as hydroxyl radicals, superoxide anions, singlet oxygen, and hydrogen peroxide, which promote oxidative degradation. Mechanistic studies based on transcriptome sequencing have shown that LIPUS significantly upregulates mitochondrial autophagy-associated proteins, promotes mitophagy, and affects mitochondrial dynamics and ROS production(Chen et al. 2022a, b). Increased levels of intracellular ROS can

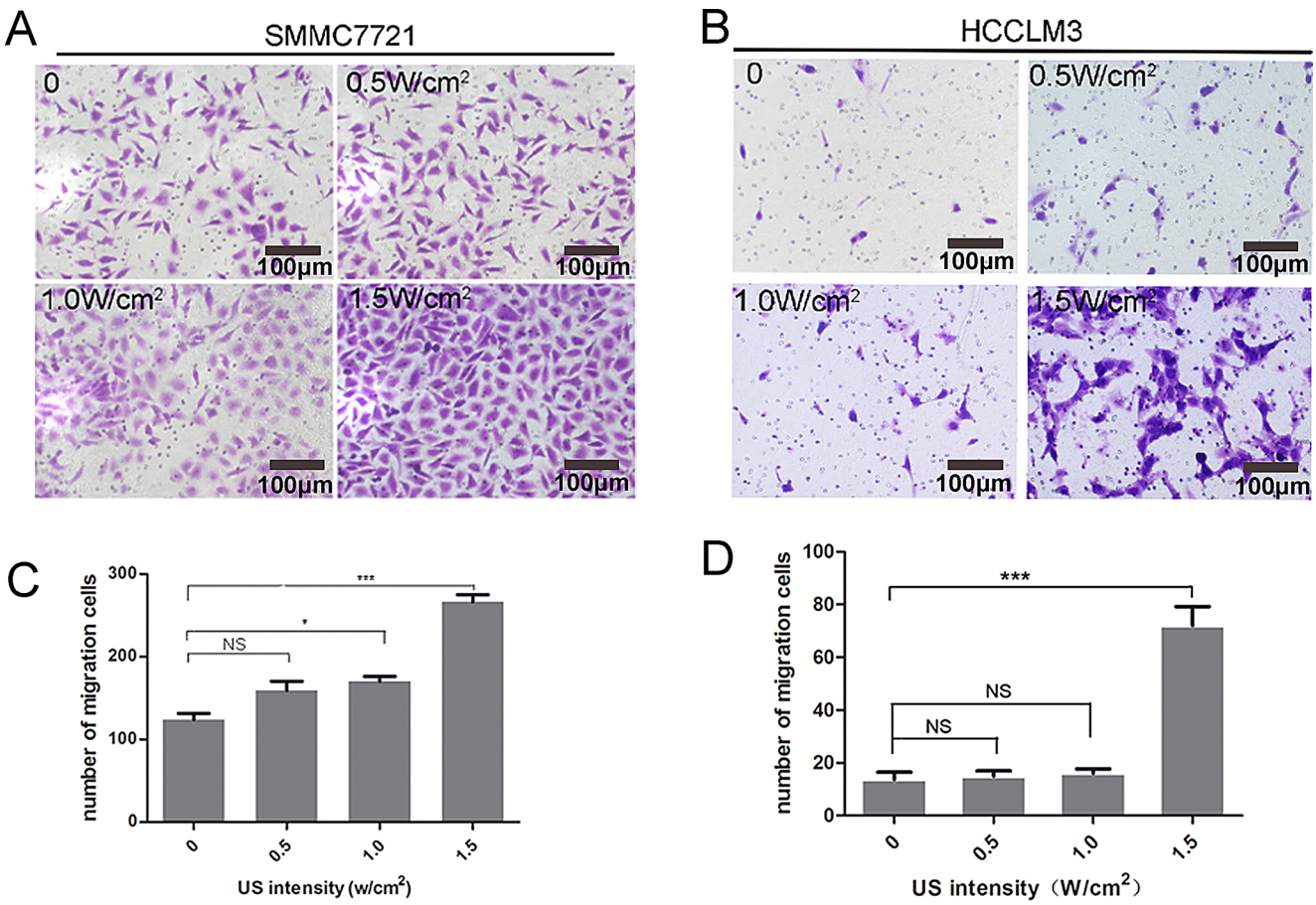

Fig. 7 LIPUS promoted the migration ability of HCCLM3 and SMMC7721. The number of migrating cells - SMMC7721 (**A**) and HCCLM3 (**B**) - passing through the transwell membrane was significantly higher in the ultrasound treatment group compared to the control group. Significant differences were observed at 1.5 W/cm^2 and 1.0 W/cm^2 for SMMC7721 (**C**) and at 1.5 W/cm^2 for HCCLM3 (**D**). *$p<0.05$ ***$p<0.001$, Scale bar = 100 μm

damage cellular structures, DNA, proteins, and lipids, ultimately leading to cell death(Singh et al. 2019). In addition, ROS can activate several pro-apoptotic proteins that induce caspase activation and apoptosis(Hong et al. 2019; Hu et al. 2023a, b). In our previous study, we demonstrated the involvement of the Ca^{2+}/mitochondrial pathway in the LIPUS-induced apoptosis of SMMC7721 cells at an intensity of 2.0 W/cm^2. In this study, we investigated whether another apoptotic mechanism involving the ROS/mitochondrial pathway is associated with LIPUS-induced apoptosis. Our results showed that exposure to LIPUS at intensities of 1.5 W/cm^2 significantly increased ROS production in both SMMC7721 and HCCLM3 cells. Mitochondrial integrity has been identified as a key factor in apoptosis induction. The reduction in MMP observed after ultrasound exposure is indicative of mitochondrial disaggregation and dysfunction. Furthermore, stimulation of ROS production following mitochondrial damage exacerbates apoptosis, as evidenced by the reduced apoptosis rates in HCC cells pretreated with the anti-apoptotic antioxidant NAC. Detection of gene expression of innate immune regulators has also verified that ROS play an important role in inducing tumor suppression and inhibiting inflammation in cells treated with LIPUS(Yang et al. 2021). The interaction between LIPUS and cancer cells results in a significant increase in ROS levels, leading to the inhibition of cancer cell growth and proliferation(Sengupta et al. 2018). While ROS-mediated mitochondrial pathway plays a significant role in LIPUS-induced apoptosis, other pathways may become more prominent at some certain energy densities, such as inhibiting the activation of EGFR and the downstream AKT/mTOR pathway(Fang et al. 2023).

LIPUS enhances cell migration and invasion in a dose-dependent manner by regulating MMPs and EMT

Some studies have suggested that LIPUS may induce metastases when it exceeds a certain intensity threshold (Li et al. 2013). Our results indicated that LIPUS irradiation induced morphological changes in adherent cells. The observed shift

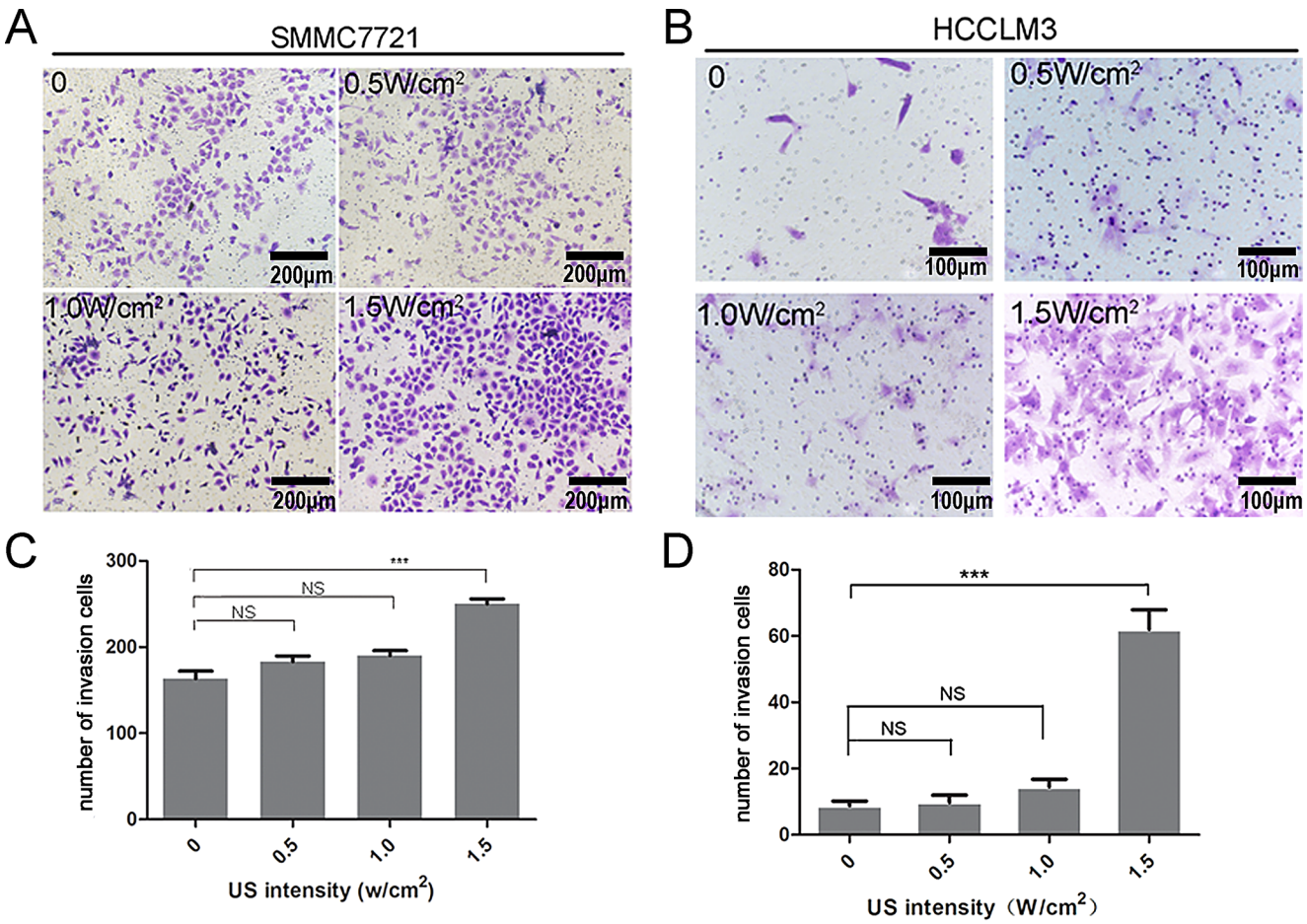

Fig. 8 LIPUS promoted the invasion ability of HCCLM3 and SMMC7721. The number of invading cells through the transwell membrane was significantly higher in the ultrasound treatment group compared to the control group (**A** and **B**). This effect was observed at an intensity of 1.5 W/cm^2 for both SMMC7721 and HCCLM3 cell lines (**C** and **D**). ***$p<0.001$, Scale bar = 200 μm for A and Scale bar = 100 μm for B

from an elliptical to a narrow shape is thought to result from LIPUS-induced disruption of intercellular junctions. Tabuchi et al. reported the induction of apoptosis in lymphoma cells after non-thermal LIPUS irradiation (0.3 W/cm^2 for 1 min) (Tabuchi et al. 2008). They observed the downregulation of genes related to cell proliferation and development, and the upregulation of genes related to cell movement, morphology, and death. Our research showed that the intensity of LIPUS positively correlated with cell attachment and migration from colonies. This underscores the need to remain vigilant regarding the potential risks associated with LIPUS, either alone or in combination, despite its ability to suppress tumor cell proliferation and induce apoptosis.

MMPs are extracellular proteins that facilitate cancer invasion and metastasis by inducing collagen degradation. Their interactions play important roles in regulating cell proliferation, migration, and invasion(Kapoor et al. 2016). MMP-2, also known as gelatinase A, is primarily synthesized by fibrous connective tissues and tumor cells. MMP-9, or gelatinase B, is predominantly produced by monocytes, macrophage polymorphonuclear leukocytes, and tumor cells, and has the ability to degrade various components of the extracellular matrix(Jiang and Li 2021). Elevated levels of MMP-2 and MMP-9 are correlated with tumor invasion, metastasis, and adverse outcomes in various malignancies. Several studies have demonstrated that MMP-2 and MMP-9 inhibition suppresses HCC metastasis(Lin et al. 2020; Wang et al. 2015; Kim et al. 2021). However, our results demonstrated that LIPUS irradiation upregulated the expression of MMP2 in both HCCLM3 and SMMC772 cells, leading us to hypothesize that MMP2 plays a pivotal role in HCC metastasis.

EMT plays a critical role in cancer metastasis and is a physiological process in which cells lose their epithelial characteristics, such as cell-cell adhesion and apical-basal polarity, while acquiring motility and mesenchymal characteristics(Nalluri et al. 2015). In the present study, classic morphological changes in cells were observed,

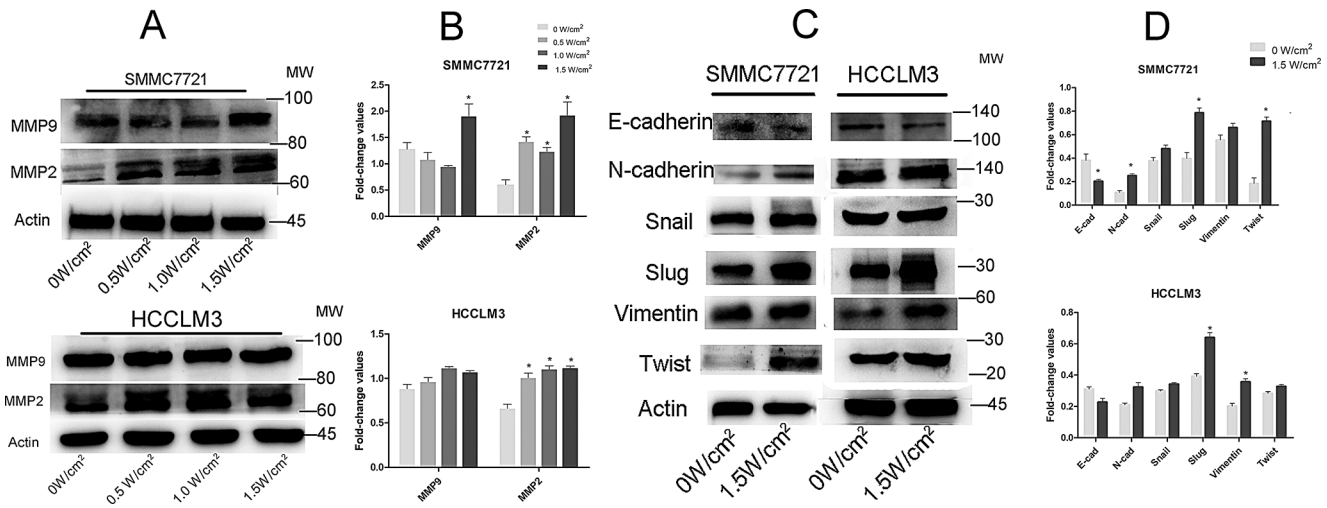

Fig. 9 LIPUS regulated the protein expression of EMT and MMPs in HCC cells. (**A**) The western blot assay revealed the protein expression of MMP2 and MMP9 in SMMC7721 and HCCLM3 cells. Compared with the control group, ultrasound treatment resulted in increased expression of MMP2, particularly at 1.5 W/cm^2 in both cell lines. The statistically significant upregulation of MMP9 was only observed in SMMC7721 cells after ultrasound treatment when compared to the control group (**B**). (**C**) Expression of EMT-associated proteins in SMMC7721 and HCCLM3 cells irradiated at 0 and 1.5 W/cm^2. In SMMC7721 cells, E-cadherin was downregulated, whereas N-cadherin, Slug, and Twist were upregulated. In HCCLM3 cells, there was a significant upregulation of Slug and vimentin (**D**). Actin was used as a reference. *$p<0.05$

along with the disruption of tight intercellular junctions. To further elucidate the underlying mechanisms, the levels of EMT-related proteins were evaluated. EMT-related protein levels were altered in response to changes in the expression of E-cadherin, which decreased, and mesenchymal-related proteins (N-cadherin and vimentin), which increased. Previous studies have suggested that the loss of E-cadherin and an increase in vimentin protein expression may lead to tumor progression, migration, and invasion(Nijkamp et al. 2011). These results suggest that LIPUS promotes HCC cell metastasis by altering the cytoskeleton via the EMT pathway. However, the observed changes were more pronounced in SMMC7721 cells than in HCCLM3 cells. This may be due to the lower metastatic potential of SMMC7721 cells than that of HCCLM3 cells, resulting in a more pronounced change in metastasis. However, we did not observe lung metastasis following LIPUS treatment in the animal experiments. This discrepancy may be attributed to differences between the in vivo and in vitro environments, as the same treatment parameters could yield varying therapeutic effects in these settings. Therefore, further investigation is warranted to explore the therapeutic effects of different ultrasound treatment parameters in vivo.

Ultrasound has demonstrated significant potential as an innovative technology for noninvasive cancer treatment, particularly with the use of LIPUS to target the stroma or enhance the efficacy of antineoplastic drugs. This approach offers a selective and noninvasive strategy that can be applied to specific areas. Our study further validated the ability of LIPUS to induce apoptosis and inhibit proliferation of HCC cells. However, we also observed that the in vitro migration and invasion capabilities of HCCLM3 and SMMC772 cells increased with higher ultrasound intensities, possibly owing to the modulation of MMPs and EMT protein expression by LIPUS. Therefore, additional research is warranted to fully understand the biological effects, establish dose standardization, evaluate the benefit-risk ratio, and assess the safety profile.

Study strengths and limitations

The strengths of this study include the systematic investigation of the effect of LIPUS on HCC and the adoption of a LIPUS intensity gradient, both of which led to the novel discovery that LIPUS may potentially promote HCC metastasis. However, this study has some limitations. First, a more comprehensive and in-depth investigation of the effects of LIPUS on proliferation, apoptosis, ROS levels, and metastasis of HCC cells is required. Further investigation into the effects of ROS accumulation on apoptosis, migration, and invasion in hepatocellular carcinoma (HCC) cells is essential to provide a more comprehensive understanding of ROS-mediated mechanisms in HCC progression. Second, the potential relationship between LIPUS-induced apoptosis and metastasis should be further explored using more sophisticated and dedicated experiments, such as RNA-seq and necrostatin-1 staining. The effects of ultrasound treatment duration, post-treatment incubation time, and therapeutic frequency on treatment efficacy, as well as their potential influence on the interplay between apoptosis and

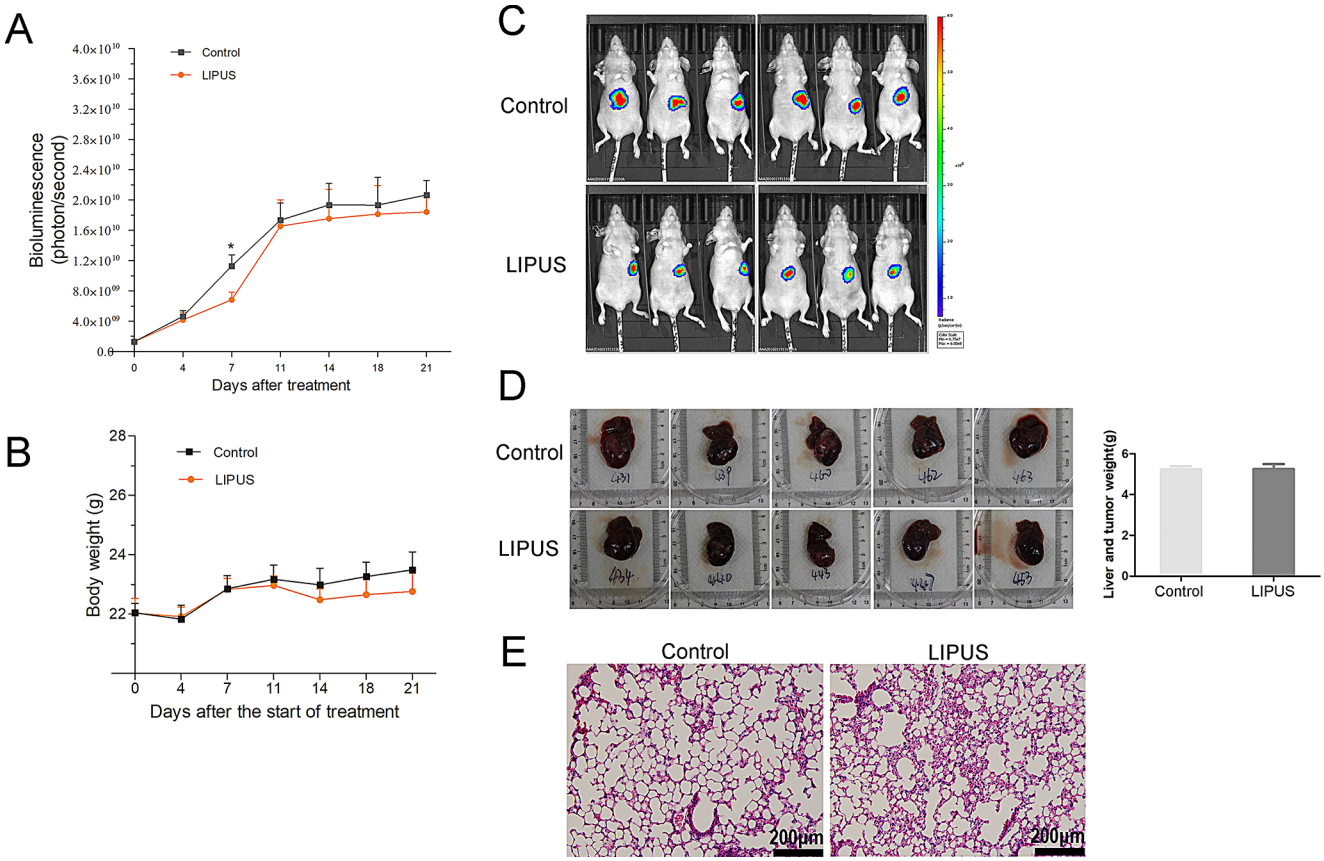

Fig. 10 The effects of LIPUS on orthotopic Hep3B-Luc tumor-bearing mice. (**A**) Bioluminescence signal intensity detection curve in mice bearing orthotopic Hep3B-Luc tumors following ultrasound treatment. Tumor growth in the ultrasound treatment group was slower than that in the control group, with a significant inhibitory effect on tumor growth observed on the 7th day. (* $P<0.05$) (**B**) The changes of body weight in mice after LIPUS treatment. (**C**) The representative fluorescence imaging map on the 7th day. (**D**) The liver images and the comparison of liver and tumor weights between the two groups of mice. In each group, one mouse died on the 20th day. (**E**) The representative HE-stained images of lung tissues

metastasis, require further investigation. Third, future studies should incorporate in vivo animal models to investigate the long-term effects and potential side effects of LIPUS, thereby providing a more comprehensive understanding and validation of the findings from this study.

Conclusion

This study provided further evidence that LIPUS promotes HCC cell apoptosis and inhibits cell proliferation. However, we also observed that the migration and invasion abilities of HCCLM3 and SMMC772 cells in vitro increased with increasing ultrasound intensity, which may be attributed to the regulation of MMPs and EMT protein expression by low-intensity ultrasound. Therefore, further research is required to fully understand its biological effects, dose standardization, benefit-risk ratio, and safety profile.

Author contributions Mingzhen Yang and Zhihui Lu designed and performed the experiments, analyzed the data, and wrote the manuscript. Bangzhong Liu and Guanghua Liu contributed to the statistical analysis, mapping, and processing of results. Mingfang Shi and Ping Wang were responsible for project administration, supervision, and validation. All authors reviewed the manuscript.

Funding This work was supported by Shanghai Research Institute of Rehabilitation Medicine Integrating Traditional Chinese and Western Medicine Project (2024XKPT20-RC1).

Data availability No datasets were generated or analysed during the current study.

Declarations

Ethical approval and consent to participate This study is approved by the Ethics Review Committee of Zhongshan Hospital, Fudan University.

Consent for publication Not applicable.

Informed consent Not applicable.

Competing interests The authors declare no competing interests.

References

Buldakov MA et al (2015) Cellular effects of low-intensity pulsed ultrasound and X-irradiation in combination in two human leukaemia cell lines. Ultrason Sonochem 23:339–346

Caillot M et al (2020) ROS Overproduction sensitises myeloma cells to Bortezomib-Induced apoptosis and alleviates tumour Microenvironment-Mediated cell resistance. Cells, 9(11)

Cao J et al (2021) Concise nanoplatform of phycocyanin nanoparticle loaded with docetaxel for synergetic Chemo-sonodynamic antitumor therapy. ACS Appl Bio Mater 4(9):7176–7185

Castaneda M et al (2022) Mechanisms of cancer metastasis. Semin Cancer Biol 87:17–31

Chen M et al (2022a) Long noncoding RNA LINC01234 promotes hepatocellular carcinoma progression through orchestrating aspartate metabolic reprogramming. Mol Ther 30(6):2354–2369

Chen Y et al (2022b) Low-Intensity pulsed ultrasound counteracts advanced glycation end Products-Induced corpus cavernosal endothelial cell dysfunction via activating mitophagy. Int J Mol Sci, 23(23)

Chrysovergis A et al (2019) Caspase complex in laryngeal squamous cell carcinoma. J BUON 24(1):1–4

Cotter TG et al (1990) Cell death via apoptosis and its relationship to growth, development and differentiation of both tumour and normal cells. Anticancer Res 10(5A):1153–1159

Evan GI, Vousden KH (2001) Proliferation, cell cycle and apoptosis in cancer. Nature 411(6835):342–348

Fang Y et al (2023) Low-intensity ultrasound combined with arsenic trioxide induced apoptosis of glioma via EGFR/AKT/mTOR. Life Sci 332:122103

Fares J et al (2020) Molecular principles of metastasis: a hallmark of cancer revisited. Signal Transduct Target Ther 5(1):28

Feril LJ et al (2005) Apoptosis induced by the sonomechanical effects of low intensity pulsed ultrasound in a human leukemia cell line. Cancer Lett 221(2):145–152

Ganesh K, Massagué J (2021) Targeting metastatic cancer. Nat Med 27(1):34–44

Gupta R, Ambasta RK, Pravir K (2021) Autophagy and apoptosis cascade: which is more prominent in neuronal death? Cell Mol Life Sci 78(24):8001–8047

Habashy KJ et al (2024) Paclitaxel and carboplatin in combination with Low-intensity pulsed ultrasound for glioblastoma. Clin Cancer Res 30(8):1619–1629

Hong M et al (2019) Acetylshikonin sensitizes hepatocellular carcinoma cells to apoptosis through ROS-Mediated caspase activation. Cells, 8(11)

Hou YJ et al (2020) Pathological mechanism of photodynamic therapy and photothermal therapy based on nanoparticles. Int J Nanomed 15:6827–6838

Hu C et al (2023a) Activation of ACLY by sect. 63 deploys metabolic reprogramming to facilitate hepatocellular carcinoma metastasis upon Endoplasmic reticulum stress. J Exp Clin Cancer Res 42(1):108

Hu Y et al (2023b) Alantolactone induces concurrent apoptosis and GSDME-dependent pyroptosis of anaplastic thyroid cancer through ROS mitochondria-dependent caspase pathway. Phytomedicine 108:154528

Huang Z et al (2020) PDLIM1 inhibits tumor metastasis through activating Hippo signaling in hepatocellular carcinoma. Hepatology 71(5):1643–1659

Ikai H et al (2008) Low-intensity pulsed ultrasound accelerates periodontal wound healing after flap surgery. J Periodontal Res 43(2):212–216

Jain A et al (2018) Ultrasound-based triggered drug delivery to tumors. Drug Deliv Transl Res 8(1):150–164

Jiang H, Li H (2021) Prognostic values of tumoral MMP2 and MMP9 overexpression in breast cancer: a systematic review and meta-analysis. BMC Cancer 21(1):149

Jiang X et al (2019) A review of Low-Intensity pulsed ultrasound for therapeutic applications. IEEE Trans Biomed Eng 66(10):2704–2718

Kapoor C et al (2016) Seesaw of matrix metalloproteinases (MMPs). J Cancer Res Ther 12(1):28–35

Kim HS et al (2021) Exosomal miR-125b exerts Anti-Metastatic properties and predicts early metastasis of hepatocellular carcinoma. Front Oncol 11:637247

Li H et al (2013) Potentiation of scutellarin on human tongue carcinoma xenograft by low-intensity ultrasound. PLoS ONE 8(3):e59473

Li R et al (2023) Sonocatalytic cancer therapy: theories, advanced catalysts and system design. Nanoscale 15(48):19407–19422

Liang S et al (2020) Recent advances in Nanomaterial-Assisted combinational sonodynamic cancer therapy. Adv Mater 32(47):e2003214

Lin XL et al (2020) Dulcitol suppresses proliferation and migration of hepatocellular carcinoma via regulating SIRT1/p53 pathway. Phytomedicine 66:153112

Liu Z et al (2019) Targeted and pH-facilitated theranostic of orthotopic gastric cancer via phase-transformation doxorubicin-encapsulated nanoparticles enhanced by low-intensity focused ultrasound (LIFU) with reduced side effect. Int J Nanomed 14:7627–7642

Loke YL et al (2023) ROS-generating alginate-coated gold nanorods as biocompatible nanosonosensitisers for effective sonodynamic therapy of cancer. Ultrason Sonochem 96:106437

Lopez W et al (2021) Ultrasound therapy, chemotherapy and their combination for prostate cancer. Technol Cancer Res Treat 20:15330338211011965

Nalluri SM, O'Connor JW, Gomez EW (2015) Cytoskeletal signaling in TGFbeta-induced epithelial-mesenchymal transition. Cytoskeleton (Hoboken) 72(11):557–569

Nijkamp MM et al (2011) Expression of E-cadherin and vimentin correlates with metastasis formation in head and neck squamous cell carcinoma patients. Radiother Oncol 99(3):344–348

Ortiz MA et al (2021) Src family kinases, adaptor proteins and the actin cytoskeleton in epithelial-to-mesenchymal transition. Cell Commun Signal 19(1):67

Pan R et al (2022) Augmenting NK cell-based immunotherapy by targeting mitochondrial apoptosis. Cell 185(9):1521–1538e18

Sawai Y et al (2012) Effects of low-intensity pulsed ultrasound on osteosarcoma and cancer cells. Oncol Rep 28(2):481–486

Scheau C et al (2019) The role of matrix metalloproteinases in the Epithelial-Mesenchymal transition of hepatocellular carcinoma. Anal Cell Pathol (Amst) 2019:p9423907

Sengupta S, Khatua C, Balla VK (2018) Vitro carcinoma treatment using magnetic nanocarriers under ultrasound and magnetic fields. ACS Omega 3(5):5459–5469

Shi M et al (2016) Low intensity-pulsed ultrasound induced apoptosis of human hepatocellular carcinoma cells in vitro. Ultrasonics 64:43–53

Singh A et al (2019) Oxidative stress: A key modulator in neurodegenerative diseases. Molecules, 24(8)

Son S et al (2020) Multifunctional sonosensitizers in sonodynamic cancer therapy. Chem Soc Rev 49(11):3244–3261

Tabuchi Y et al (2008) Genetic networks responsive to low-intensity pulsed ultrasound in human lymphoma U937 cells. Cancer Lett 270(2):286–294

Tamboia G et al (2022) A comparative analysis of low intensity ultrasound effects on living cells: from simulation to experiments. Biomed Microdevices 24(4):35

Tan Y et al (2018) Loss of nucleolar localization of NAT10 promotes cell migration and invasion in hepatocellular carcinoma. Biochem Biophys Res Commun 499(4):1032–1038

Tang J, Guha C, Tome WA (2015) Biological effects induced by Non-thermal ultrasound and implications for cancer therapy: A review of the current literature. Technol Cancer Res Treat 14(2):221–235

Urita A et al (2013) Effect of low-intensity pulsed ultrasound on bone healing at osteotomy sites after forearm bone shortening. J Hand Surg Am 38(3):498–503

Vogel A et al (2022) Hepatocellular carcinoma. Lancet 400(10360):1345–1362

Wang YH et al (2015) BRD4 induces cell migration and invasion in HCC cells through MMP-2 and MMP-9 activation mediated by the Sonic Hedgehog signaling pathway. Oncol Lett 10(4):2227–2232

Xin Z et al (2016) Clinical applications of low-intensity pulsed ultrasound and its potential role in urology. Transl Androl Urol 5(2):255–266

Xue Q et al (2022) Regulation of mitochondrial network homeostasis by O-GlcNAcylation. Mitochondrion 65:45–55

Yang Q et al (2021) Ultrasound May Suppress Tumor Growth, Inhibit Inflammation, and Establish Tolerogenesis by Remodeling Innatome via Pathways of ROS, Immune Checkpoints, Cytokines, and Trained Immunity/Tolerance. J Immunol Res, 2021: p. 6664453